Proceedings World Geothermal Congress 2015
Melbourne, Australia, 19-25 April 2015

Forward Induced Seismic Hazard Assessment (FISHA) Based on a Hydromechanical Coupled Fracture Mechanics Earthquake Model – The Case of Synthetic Induced Seismicity Catalogue Including Aseismic Displacements of Pre-Existing Fractures

Amir H. Hakimhashemi, JeoungSeok Yoon, Oliver Heidbach, Arno Zang, Gottfried Grünthal, Günter Zimmermann

GFZ German Research Centre for Geosciences, Section 2.6 Seismic Hazard and Stress Field,

Telegrafenberg, Potsdam 14473, Germany

hakim@gfz-potsdam.de

Keywords: Geothermal reservoir, induced seismicity, seismic hazard, hydromechanical model, fracture mechanics

ABSTRACT

The occurrence of an M_w 3.2 induced seismic event in 2006 during the injection of fluid at the Basel geothermal site in Switzerland initiated an on-going discussion on the potential hazard and risk of hydraulic stimulation in Europe. So far, development of mitigation strategies of induced Seismic Events of Economic Concern (SEECo) has become an important issue. Statistical methods have been developed to understand the induced seismicity from which appropriate strategy for mitigating effect of SEECo can be established. However, all these methods require catalogues of monitored seismicity. Therefore, they cannot deliver *a priori* strategies for stimulation treatment.

Here we present the Forward Induced Seismic Hazard Assessment (FISHA). This procedure converts the output of a hydromechanical coupled and fracture mechanics based model into probabilistic seismic hazard of induced seismicity in terms of time-dependent occurrence rate of induced seismic events. FISHA is applied to the simulation results of various stimulation scenarios, where injection flow rate, duration and style of injection, as well as reservoir parameters are varied. The geothermal reservoir is modelled using a discrete element fracture network that is coupled to a routine of viscous fluid flow in porous media generating flow-driven failure of rock matrix and pre-existing fractures in Mode I (tensile) and Mode II (shear). The output is a synthetic seismicity catalogue. This catalogue includes hypocentre, occurrence time and magnitude of induced seismic events. The synthetic catalogue is then used to determine the magnitude completeness M_c and to estimate the time-dependent parameters *a* and *b* of the Gutenberg-Richter frequency-magnitude relation using statistical methods. These parameters are then applied to estimate the time-dependent occurrence rate of SEECo for each stimulation scenario. In this way, we can evaluate the stimulation scenarios in terms of hazard according to the corresponding rate of SEECo. The advantage of FISHA is then the assessment of the occurrence rate of SEECo resulting from various stimulation scenarios, which gives *a priori* information to operator how to mitigate the risk of occurrence of SEECo.

1. INTRODUCTION

Geothermal energy is known as a mode of renewable energy resources which can play an important role in replacing fossil and nuclear energy in the future. A regular method to profit the energy of geothermal reservoirs is to enhance permeability of the reservoir by stimulating rock mass through high-pressure fluid injection. This method is known as hydraulic fracturing (Hubbert and Willis, 1957). However, fluid injection into the rock mass induces seismicity, which can become a problem by triggering larger events (Evans et al., 2012; Majer et al., 2007, 2012; Grünthal, 2013). Although such events are generally of moderate magnitudes, they can cause damage to the surface structures. For that reason we use the term "Seismic Events of Economic Concern, SEECo" to refer to these kinds of events (Grünthal, 2013; Hakimhashemi et al., 2014a). Such induced SEECo occurred, e.g. in 2006 at the geothermal site in Basel, Switzerland. The occurrence of a 2.9 ML during the stimulation of the geothermal reservoir led to an enforced shut-in of the fluid injection. However, occurrence of two following SEECo, i.e. a 2.7 and a 3.4 ML events, on the same day of shut-in resulted in complete desistance of the reservoir (Häring et al., 2008; Deichmann and Ernst, 2009; Deichmann and Giardini, 2009). Also in 2009 at the geothermal site in Landau, Germany, a 2.6 Mw event occurred shortly after shut-in (Grünthal, 2013). The mentioned events alongside other similar cases of occurrence of SEECo in geothermal reservoirs strengthened a wide discussion on the hazard and risk due to activities at geothermal reservoirs. It should be mentioned that the characterisation of the SEECo, i.e. the magnitude, directly depends on the local socio-economical parameters which can be considered as the maximum acceptable magnitude of induced events from the local society and government. For example, magnitude level of SEECo can vary for an area with relatively low level of natural seismicity, e.g. Basel in Switzerland, compared to higher level of natural seismicity area, e.g. Reykjavik in Iceland. However, regardless of local settings of magnitude of the SEECo, strategies of mitigation of the occurrence rate of SEECo during hydraulic stimulation and operation of geothermal reservoirs are required.

So far, various mitigation strategies have been suggested and partly applied. The traffic light system by Bommer et al. (2006), a physics-based model to describe the induced seismicity in a reservoir by Shapiro et al. (2010) and Dinske and Shapiro (2013), as well as a statistical model by Barth et al. (2013) use monitored induced seismicity to perform mitigation strategies (Hakimhashemi et al., 2014a). Although analysing monitored induced seismicity can help understanding the processes leading to occurrence of SEECo, these models are bound to certain local settings of the monitored reservoir and cannot deliver *a priori* mitigation strategies.

Geomechanical numerical models, as an alternative way, can be *a priori* applied considering physical rules including the thermal and/or hydromechanical coupled processes (e.g. Bruel, 2007; Kohl and Mégel, 2007; Rutqvist et al., 2007; Altmann et al., 2010; Baisch et al., 2010; Schoenball et al., 2010; McClure and Horne, 2011). In general, this type of models transfers spatio-temporal changes in the stress field of a site. In particular, an extra procedure is required to translate the spatio-temporal stress changes in

form of seismicity (Bruel, 2007; Zang et al., 2013; Yoon et al., 2014). However, the output of the geomechanical model, either as spatio-temporal stress changes or as simulated induced seismicity, still needs to be converted to the potential occurrence rate of SEECo in order to define mitigation strategies.

This procedure has been done under a work flow known as Forward Induced Seismic Hazard Assessment, FISHA (Hakimhashemi et al., 2014a). FISHA uses the output of a geomechanical numerical model and transforms it to the potential occurrence rate of SEECo using probabilistic-statistical methods. In fact, the FISHA combines geomechanical numerical models with probabilistic-statistical models. Therefore, it has not only the capacity of an *a priori* procedure (based on the geomechanical numerical modelling part), but also the capability to test strategies to mitigate the occurrence rate of SEECo.

The FISHA workflow is planned for two branches corresponding to two types of outputs of the geomechanical numerical models, i.e. the spatio-temporal changes in the stress field and the simulated induced seismicity catalogue (Hakimhashemi et al., 2013). Both branches have been exemplified and the results have been published in Hakimhashemi et al. (2014a,b) corresponding to (a) the simulated induced seismicity catalogue and (b) the changes in the stress field, respectively.

Hakimhashemi et al. (2014a) focussed on the induced seismicity generated by a hydro-geomechanical model of Yoon et al. (2014), comparing the induced seismic hazard, i.e. the potential occurrence rate of events with magnitudes larger or equal to 1.5, calculated for four different injection scenarios. The induced seismic hazard was estimated using induced seismicity catalogues including co-seismic events converted from Mode I tensile and Mode II shear failures. However, slip of pre-existing fractures was excluded in estimation of potential induced seismic hazard. The aim of the current study is, therefore, to analyse the effect of such slip of pre-existing fractures on the potential induced seismic hazard. We reinvestigate the injection type1 in Hakimhashemi et al. (2013), i.e. the stepwise sequential high flow rate injection. Thirty pre-existing fractures are considered which are represented by collection of 693 smooth joint contact planes. The shear displacements of each smooth joint contact plane are registered every 20 seconds and the moment magnitudes are calculated. Using this slip event catalogue in addition to the failure event catalogue (Hakimhashemi et al., 2013) the magnitude completeness (M_c), as well as the a and b parameters of the Gutenberg-Richter frequency-magnitude distribution are calculated for each 20 second time interval. Finally, using the estimated parameters a, b and M_c the potential occurrence rate of SEECo is calculated.

In this study the magnitude assigned to the SEECo is considered as larger or equal to 1.5 similar to the study by Hakimhashemi et al. (2014a). Finally the results are compared with the results according to the case of failure events as well as the larger magnitude events in the catalogue.

2. FORWARD INDUCED SEISMIC HAZARD ASSESSMENT, FISHA WORKFLOW

As mentioned in the previous section, FISHA is a workflow which combines geomechanical-numerical models and probabilistic-statistical model in order to calculate the seismic hazard. The FISHA workflow is subdivided into two branches, each branch corresponding to a general type of geomechanical-numerical model (Fig. 1).

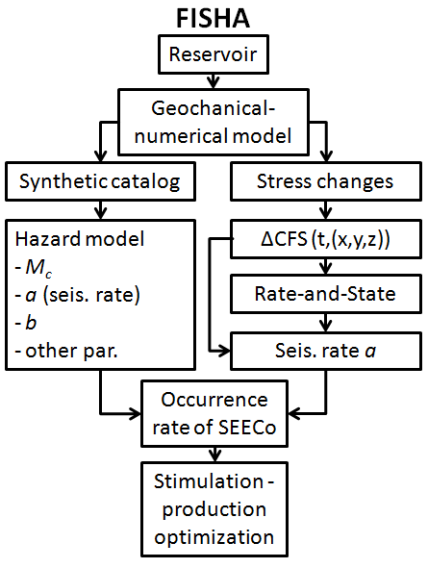

Figure 1: Structure of the Forward Induced Seismic Hazard Assessment (FISHA) including two branches using two different types of geomechanical-numerical models, left branch based on synthetic catalogues and the other based on spatio-temporal stress changes, i.e. Coulomb Failure Stress changes ΔCFS(t,(x,y,z)). a, b are the parameters of the frequency-magnitude distribution and M_c is the magnitude completeness. SEECo are Seismic Events of Economic Concerns.

One branch is dedicated to the type of geomechanical-numerical models which deliver synthetic induced seismicity catalogue as the main output (Zang et al., 2013; Yoon et al., 2014). The seismicity catalogue is then used to estimate the seismic hazard, which is defined here as the potential occurrence rate of SEECo. For that reason, the frequency-magnitude a and b parameters as well as the magnitude of completeness, M_c, are estimated for the synthetic seismicity catalogue. Finally the parameters a, b and M_c are applied

to a statistical model to calculate the potential occurrence rate of SEECo. More details and application of this branch of FISHA can be found in Hakimhashemi et al. (2014a).

The focus of the other branch of FISHA is the type of geomechanical-numerical models which deliver the spatio-temporal stress changes in the reservoir as main output. The spatio-temporal stress changes are converted to the seismicity rate using a Rate-and-State type models (Dieterich, 1994). This branch of FISHA was explained and applied in Hakimhashemi et al. (2014b).

3. GEOMECHANICAL-NUMERICAL MODEL

The geomechanical-numerical model we used is called Discrete Bonded Particle Model (DBPM). A commercial code Particle Flow Code 2D (PFC2D) is used in which fluid flow algorithm and seismicity algorithm are additionally implemented (Yoon et al., 2013a, b). The former enables modelling of flow of viscous fluid in porous media. Flow volume and pressure driven failure of rock matrix and pre-existing fractures are modelled in two Modes: Mode I tensile and Mode II shear. Upon failure which is a bond breakage at particle-particle contact, stored strain energy is released and propagates as a seismic wave. The implemented seismicity-computing algorithm (Yoon et al., 2013a, b) which is a modified form of Hazzard and Young (2002, 2004) computes moment tensors of the Mode I and II failures from which seismic moment (M_0) and moment magnitude (M_w) are computed. Such seismicity computed from bond breakage (failure) is referred to coseismic events. In addition to this, slip (shear displacement) of pre-existing fractures are monitored and used to calculate the M_0, using the equation of $M_0 = GAd$, where G is shear modulus (= 30 GPa), A is rupture area (m^2), and d is shear displacement (m). Such slip events are referred to aseismic events.

Figure 2 shows the 2D discrete element fracture network model representing a hard rock geothermal reservoir with pre-existing fractures. For intact rock matrix, strength and deformation attributes are assigned to resemble the crystalline rock mass of Soultz-sous-Forêts, France. Mechanical and hydromechanical coupled parameters for the discrete fractures are also taken from a crystalline environment from the Forsmark site, Sweden. The modelling parameters can be found in Yoon et al. (2013a, their Table 1) and in more detail in Zang et al. (2013, in supplementary material). The model is calibrated against Soultz granite properties, but not validated against observed seismicity catalogue because of 2D nature of the model. Failure of rock matrix and pre-existing fractures is governed by the Mohr-Coulomb criterion (Labuz and Zang, 2012).

The constructed model is 2 km x 2 km in size and subjected to compressive in-situ stresses with S_H = 75 MPa and S_h = 60 MPa. The applied boundary stresses as maximum and minimum horizontal stresses (S_H, S_h) are taken from the stress-depth relation of Soultz site (Cornet et al., 2007, their equations 1a and 1b) at 4 km depth. At the injection point at the centre of the model we test different injection scenarios. The outputs of the model are distribution of fluid pressure in space and time and catalogues of the induced seismic events, with occurrence time, location and magnitude. The injection is controlled by the flow rate in l/s over time. Details on the injection scenarios are given in the section where the results of the FISHA workflow are presented.

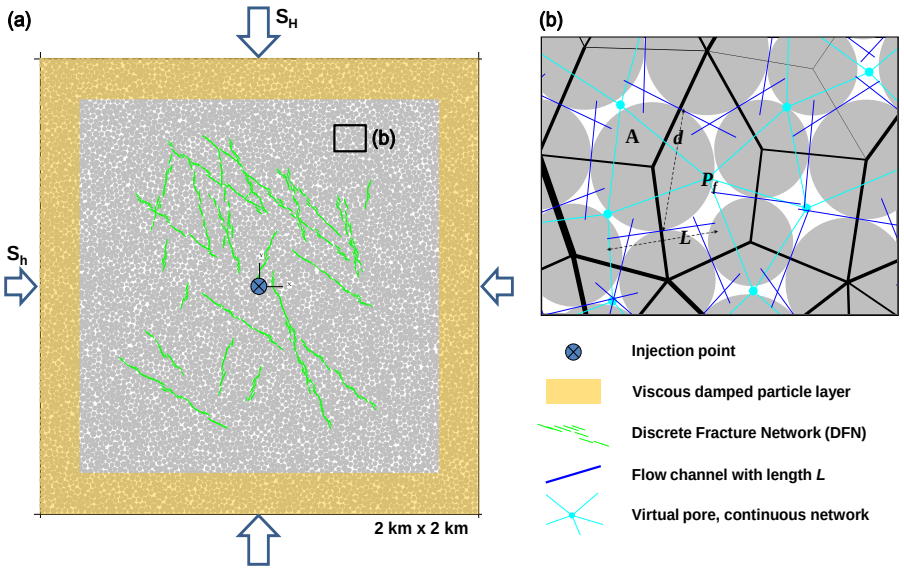

Figure 2: (a) Synthetic geothermal reservoir in 2 km x 2km size at 4 km depth with embedded discrete fractures and subjected to differential in situ stress of S_H = 75 MPa and S_h = 60 MPa, (b) Zoom-in view of the boxed area showing concept of hydro-mechanical coupling algorithm. Each black polygon defines the void spaces in which virtual pores are placed at their centres which can store fluid pressure. Fluid flow between pores are modelled through the flow channels (blue) governed by pressure gradient, fluid viscosity, and aperture.

4. SEISMIC HAZARD MODEL

In this study the seismic hazard is defined as the potential occurrence rate of SEECo, which can be calculated using the parameters *a* and *b* of the frequency-magnitude relation (Gutenberg and Richter, 1956) as

$$\log N = a - b(M - M_c), \quad M \geq M_c , \tag{1}$$

where N is the number of events of magnitude M ($M \geq M_c$), M_c is the magnitude of completeness which shows from which magnitude all events are included in the catalogue, and a and b are the model parameters. Equation (1) leads to an exponential distribution for the magnitudes with density function as

$$f(m) = \begin{cases} 0 & m < M_c \\ \beta e^{-\beta(m-M_c)} & m \geq M_c \end{cases}, \tag{2}$$

where $\beta = b \bullet \ln 10$.

To estimate M_c a maximum likelihood estimator (Stigler, 2007) has been applied. However, in many cases of seismicity catalogues/datasets, where the magnitude data are not well-behaved, a local maximum likelihood cannot be found. For such cases a method of maximum curvature (Wiemer & Wiess, 2000) has been applied. In both methods M_c has been estimated, for a given set of magnitudes, among a potential set of possible M_c. Then β can be estimated given a possible M_c. The logarithmic maximum likelihood function of parameter β given a possible M_c can be written as

$$l(\beta) = \ln\left(\prod_{m \in M} f(m)\right) = \sum_{m \in M} \ln \beta e^{-\beta(m-M_c)} = \sum_{m \in M} \ln \beta - \sum_{m \in M} \beta(m - M_c), \tag{3}$$

where M is the set of magnitudes $\geq M_c$. $\hat{\beta}$, i.e. the estimation of β, can be obtained by solving the equation $\frac{dl(\beta)}{d\beta} = 0$ over β which leads to

$$\hat{\beta} = \frac{1}{(\overline{m} - M_c)}, \qquad \overline{m} = mean\{m \mid m \in M\}. \tag{4}$$

Using $\hat{\beta}$, $l(\hat{\beta})$ can be calculated for each possible M_c. Then the optimal M_c can be selected as, either as the M_c corresponding to the maximum $l(\hat{\beta})$ over M_c for the case of maximum likelihood, or the M_c corresponding to the maximum curvature of the $l(\hat{\beta})$ over M_c. The parameter β, and consequently parameter b, can be then selected according to the selected M_c. Parameter a is considered equivalent to the rate of events with magnitudes $\geq M_c$.

The final step is to calculate the hazard, i.e. the potential occurrence rate of SEECo, which is considered here as the potential rate of events with magnitudes ≥ 1.5 (Hakimhashemi et al., 2014a). According to equation (2) the probability that an event of magnitude m_g ($m_g \geq M_c$) or larger occurs can be written as

$$\Pr(M \geq m_g \mid M \geq M_c) = e^{-\beta(m_g - M_c)}. \tag{5}$$

Then the potential occurrence rate of m_g can be calculated using the following equation

$$\vartheta = a \Pr(M \geq m_g \mid M \geq M_c). \tag{6}$$

As mentioned in the previous section, the aseismic event catalogue which are pre-existing fracture slip has been generated for 20 seconds intervals. These intervals have been also considered for the combined catalogue of the coseismic and aseismic catalogues together. Therefore, for each 20 seconds period there is a set of events occurring in the same 20 seconds interval. The hazard model has been then applied to each set of events corresponding to each 20-second interval. For 9000 such 20-second intervals (covering 50 hours beginning from the starting of injection), the parameters M_c, a and b as well as their confidence intervals have been calculated for each set of 20 second interval, separately. Using the estimated parameters the hazard, i.e. the potential occurrence rate of events with magnitudes ≥ 1.5, has been calculated in 20 seconds intervals.

5. APPLICATION OF THE MODEL ON THE CATALOGUE

The hazard model has been applied to the combined catalogue of the coseismic and aseismic events catalogues. The combined catalogue covers a 50 hour period starting from the beginning of the injection (the injection duration is around 6.5 hours). This catalogue is subdivided into 9000 sub-dataset of events separated for each 20 second period. The hazard model has been applied to each sub-dataset. Fig. 3 top shows the injection rate in litre per second (black curve and gray area) and the simulated downhole pressure in MPa (red curve). Fig. 3 middle shows the maximum observed magnitude in the combined simulated catalogue for each 20 second interval (blue small circles) and the estimated magnitude of completeness, M_c, (black small crosses) also for each 20 second interval. Fig. 3 bottom demonstrates the parameter b (black curve) as well as the hazard, i.e. the potential occurrence rate of events with magnitudes ≥ 1.5 (red curve) for each 20 second interval.

Table 1 shows the maximum and minimum values of the estimated parameters a, b and M_c (among all 20 second intervals, i.e. 9000 intervals) as well as their confidence intervals.

The reliability of the estimated parameters has been analysed using a variation criterion which is calculated using

$$\frac{(\text{estimation} - \text{lower confidence bound}) + (\text{upper confidence bound} - \text{estimation})}{2 * \text{estimation}}.$$

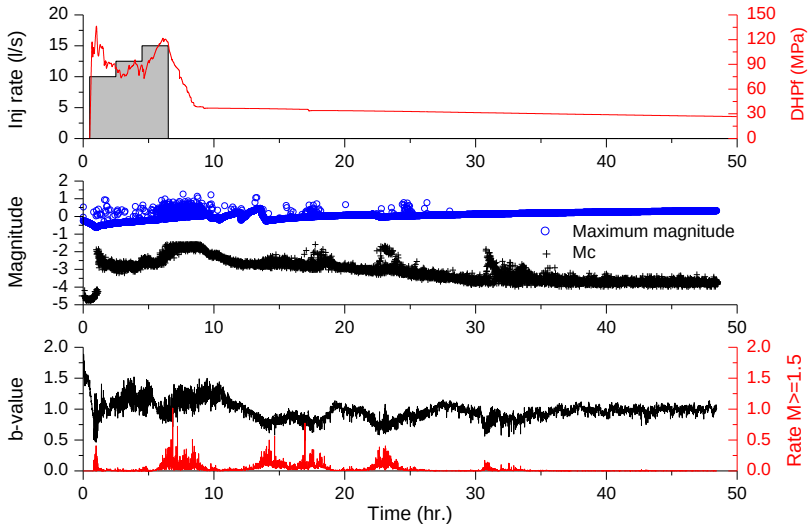

Figure 3: Top: Applied injection rate in *l/s* (black curve and gray area) and the simulated downhole pressure in MPa (red curve). Middle: Maximum observed magnitudes (blue circles) and estimated magnitudes of completeness M_c (black crosses) for each 20second period. Bottom: Estimated parameter *b* of the frequency-magnitude distribution (black curve) and the estimated hazard, i.e. the potential occurrence rate of seismic events with magnitudes ≥ 1.5 (red curve) for each 20 second period.

Fig. 4 shows the histogram of the variation criterions for the parameters *a* (left subfigure), *b* (middle subfigure) and M_c (right figure) for the 9000 time periods. The results show a high level of reliability for parameters *b* and M_c, and a good level of reliability for the parameter *a*.

Table 2: Maximum and minimum estimated values as well as the 95% confidence intervals of parameters *a*, *b* and M_c among all 20 second intervals, i.e. 9000 intervals.

Parameter	*A*		*b*		M_c	
	min	max	Min	max	min	Max
Estimation	32 + [0,5]	475 + [-3,2]	0.465 + [-0.006,0.004]	1.888 + [-0.014,0.011]	-4.71 + [-0.01,0.06]	-1.51 + [0,0]

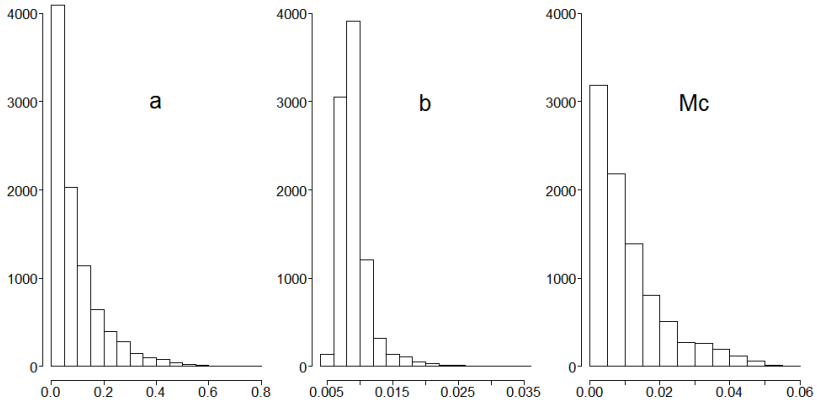

Figure 4: Histograms of variation criteria, i.e. (upper bound – lower bound)/(2*estimation), for the parameters *a* (left), *b* (middle) and M_c (right) for the 9000 time periods.

6. DISCUSSION

According to Fig. 3, the hazard curve (red curve in the bottom subfigure), i.e. the potential occurrence rate of events with magnitudes ≥ 1.5, is generally in a good agreement with the maximum magnitude events (blue circles in the middle subfigure). There are two delayed swarms after shut-in, i.e. one in 15-20 hr range and the other at 25 hr, which occurred due to the migration of the pressurized fluid. A single case where the changes in hazard and the maximum events are not completely simultaneous happens after 22.5 hr when the increase in hazard occurs before the seismic swarm appears.

The maximum hazard is estimated for the seismic event swarm during and shortly after shut-in. The hazard curve responds to the *b*-value curve reversely, i.e. the hazard increases when the *b*-value decreases and vice versa.

The hazard, in this study, has been calculated based on 20 second periods. The reason for the 20 second duration is the hypothesis that the average duration of a single displacement on a pre-existing fracture takes 10 to 20 seconds. However, a method for an exact calculation of each single displacement on each zone is missing.

The maximum hazard calculated using the combined coseismic and aseismic events catalogues in this study (equal to 1.017 for 20 second rate) is higher than the one using only the coseismic catalogue (equal to 10.15 hourly rate, according to the results of the type 1 injection in Hakimhashemi et al., 2014a). This large difference is expected according to the amount of energy release corresponding to the more than 2 millions aseismic displacements with magnitudes in range of [-4.71,0.45] occurring in 693 smooth planes in pre-existing fractures.

7. CONCLUSIONS

The FISHA workflow (Fig. 1) links the results of geomechanical-numerical models with time-dependent hazard assessment of induced seismicity. We applied FISHA using a new geomechanical-numerical model which considers pre-existing fractures and delivers, not only the usual coseismic induced seismicity catalogue (including shear and tensile events), but also an additional aseismic displacements on the pre-existing fractures. Using this combined aseismic and coseismic catalogue, the parameters *a* and *b* of the frequency-magnitude distribution, as well as the parameter M_c (magnitude completeness) and their uncertainties were estimated. Using these parameters the hazard, i.e. the potential occurrence rate of events with magnitudes ≥ 1.5, was calculated for 20 second periods.

The results of the hazard are, in the most periods, in good agreement with the maximum magnitudes in each 20 second period. The hazard also shows a diverse relation to the parameter *b*, i.e. when *b* decreases the hazard increases and vice versa.

Finally, the hourly maximum hazard calculated using the combined coseismic and aseismic catalogue is much larger than the case of using only the usual coseismic catalogue. This large difference is an evidence for the necessity of considering the aseismic displacements in the pre-existing fractures as a part of the induced seismicity catalogues.

ACKNOWLEDGEMENTS

Development of the geomechanical-numerical model was supported by a project funded by the German Federal Ministry of Economic Affairs and Energy (grant no. 0325451C).

REFERENCES

Altmann, J., Müller, T., Müller, B., Tingay, M., and Heidbach, O.: Poroelastic Contribution to The Reservoir Stress Path, *Int J Rock Mech Min*, **47(7)**, (2010), 1104–1113.

Baisch, S., Voros, R., Rothert, E., Stang, H., Jung, R., Schellschmidt, R.: A Numerical Model for Fluid Injection Induced Seismicity at Soultz-sous-Forêts, *Int J Rock Mech Min*, **47(3)**, (2010), 405–413.

Barth, A., Wenzel, F., and Langenbruch, C.: Probability of earthquake occurrence and magnitude estimation in the post shut-in phase of geothermal projects, *J Seismol*, **17(1)**, (2013), 5-11.

Bommer, J.J., Oates, S., Cepeda, J.M., Lindholm, C., Bird, J., Torres, R., Marroquin, G., and Rivas, J.: Control of hazard due to seismicity induced by a hot fractured rock geothermal project, *Eng Geol*, **83**, (2006), 287–306.

Bruel, D.: Using the migration of induced seismicity as a constraint for fractured hot dry rock reservoir modelling, *Int J Rock Mech Min*, **44**, (2007), 1106–1117.

Cornet, F.H., Bèrard, Th., and Bourouis, S.: How close to failure is a granite rock mass at a 5 km depth? *Int J Rock Mech Min*, **44(1)**, (2007), 47–66.

Deichmann, N., and Ernst, J.: Earthquake focal mechanisms of the induced seismicity in 2006 and 2007 below Basel (Switzerland), *Swiss J Geosci*, **102**, (2009), 457-466.

Deichmann, N., and Giardini, D.: Earthquakes induced by the stimulation of an enhanced geothermal system below Basel (Switzerland), *Seismol Res Lett*, **80(5)**, (2009), 784-798.

Dieterich, J.: A constitutive law for rate of earthquake production and its application to earthquake clustering, *J Geophys Res*, **99(B2)**, (1994), 2601–2618.

Dinske, C., and Shapiro, S.: Seismotectonic state of reservoirs inferred from magnitude distributions of fluid-induced seismicity, *J Seismol*, **17(1)**, (2013), 13-25.

Evans, K.F., Zappone, A., Kraft, T., Deichmann, N., and Moia, F.: A survey of the induced seismic response to fluid injection in geothermal and CO2 reservoirs in Europe, *Geothermics*, **41**, (2012), 30-54.

Grünthal, G.: Induced seismicity related to geothermal projects versus natural tectonic earthquakes and other types of induced seismic events in Central Europe, *Geothermics*, (2013), DOI: 10.1016/j.geothermics.2013.09.009.

Hakimhashemi, A. H., Yoon, J. S., Heidbach, O., Zang, A., and Grünthal, G.: FISHA – Forward induced seismic hazard assessment application to synthetic seismicity catalog generated by hydrulic (sic) stimulation modeling, *Proceedings*, 38th Workshop on Geothermal Reservoir Engineering, Stanford University, Stanford, CA (2013).

Hakimhashemi, A. H., Yoon, J. S., Heidbach, O., Zang, A., and Grünthal, G.: Forward induced seismic hazard assessment: application to a synthetic seismicity catalogue from hydraulic stimulation modeling, *J Seismol*, (2014a), DOI: 10.1007/s10950-014-9439-y

Hakimhashemi, A.H., Schoenball, M., Heidbach, O., Zang, A., Grünthal, G.: Forward modelling of seismicity rate changes in georeservoirs with a hybrid geomechanical-statistical prototype model, *Geothermics*, (2014b), DOI: 10.1016/j.geothermics.2014.01.001.

Häring, M.O., Schanz, U., Ladner, F., and Dyer, B.C.: Characterisation of the Basel 1 enhanced geothermal system, *Geothermics*, **37(5)**, (2008), 469–495.

Hazzard, J.F., and Young, R.P.: Moment Tensors and Micromechanical Models, *Tectonophysics*, **356**, (2002), 181-197.

Hazzard, J.F., and Young, R.P.: Dynamic Modelling of Induced Seismicity, *Int J Rock Mech Min*, **41(8)**, (2004), 1365-1376.

Hubbert, M.K., and Willis, D.G.: Mechanics of Hydraulic Fracturing. *Trans. AIME*, **210**, (1957), 153-166.

Kohl, T., and Megel, T.: Predictive modeling of reservoir response to hydraulic stimulations at the European EGS site Soultz-sous-Forets, *Int J Rock Mech Min*, **44(8)**, (2007), 1118–1131.

Labuz, J.F., and Zang, A.: Mohr-Coulomb failure criterion, *Rock Mech Rock Eng*, **45**, (2012), 975-979.

Majer, E.L., Baria, R., Stark, M., Oates, S., Bommer, J., Smith, B., and Asanuma, H.: Induced seismicity associated with enhanced geothermal system, *Geothermics*, **36**, (2007), 185–222.

Majer, E., Nelson, J., Robertson-Tait, A., Savy, J., and Wong, I.: Protocoll for addressing induced seismicity associated with enhanced geothermal systems, *U.S. Department of Energy*, (2012), DOE/EE-0662.

McClure, M.W., and Horne, H.N.: Investigation of injection-induced seismicity using a coupled fluid flow and rate and state friction model, *Geophysics*, **76(6)**, (2011), WC183-WC200.

Rutqvist, J., Birkholzer, J., Cappa, F., and Tsang, C-F.: Estimating maximum sustainable injection pressure during geological sequestration of co2 using coupled fluid flow and geomechanical fault-slip analysis, *Energy Conversion and Management*, **48**, (2007), 1798–1807.

Schoenball, M., Müller ,T.M., Müller, B., and Heidbach, O.: Fluid-induced microseismicity in pre-stressed rock masses, *Geophys J Int*, **180**, (2010), 113–119.

Shapiro, S., Dinske, C., Langenbruch, C., and Wenzel, F.: Seismogenic Index and Magnitude Probability of Earthquakes Induced during Reservoir Fluid Stimulations, *Leading Edge*, **29(3)**, (2010), 304–309.

Yoon, J.S., Zang, A., and Stephansson, O.: Hydro-Mechanical Coupled Discrete Element Modeling of Geothermal Reservoir Stimulation and Induced Seismicity, *Proceedings*, 3rd Sino-German Conference on Underground Storage of CO2 and Energy, Goslar, Germany (2013a).

Yoon, J.S., Zang, A., and Stephansson, O.: Simulation of hydraulic stimulation of fractured reservoir and induced seismicity using discrete element-fracture network model, *Proceedings*, 38th Workshop on Geothermal Reservoir Engineering, Stanford University, Stanford, CA (2013b).

Yoon, J.S., Zang, A., and Stephansson, O.: Numerical investigation of optimized stimulation of intact and naturally fracture deep geothermal reservoirs using hydro-mechanical coupled discrete particles joints model, *Geothermics*. (2014), DOI: 10.1016/j.geothermics.2014.01.009.

Zang, A., Yoon, J.S., Stephansson, O., and Heidbach, O.: Fatigue hydraulic fracturing by cyclic reservoir treatment enhances permeability and reduces induced seismicity, *Geophys J Int*, **195**, (2013), 1282–1287.